

ADRIANO HENRIQUE GONÇALVES PIMENTEL

**PYROCLASTIC DENSITY CURRENT-FORMING  
ERUPTIONS ON FAIAL AND TERCEIRA ISLANDS, AZORES**

*ERUPÇÕES FORMADORAS DE PRODUTOS PIROCLÁSTICOS  
DE FLUXO NAS ILHAS FAIAL E TERCEIRA, AÇORES*



UNIVERSIDADE DOS AÇORES  
DEPARTAMENTO DE GEOCIÊNCIAS  
2015

**ADRIANO HENRIQUE GONÇALVES PIMENTEL**

**PYROCLASTIC DENSITY CURRENT-FORMING  
ERUPTIONS ON FAIAL AND TERCEIRA ISLANDS, AZORES**

*ERUPÇÕES FORMADORAS DE PRODUTOS PIROCLÁSTICOS  
DE FLUXO NAS ILHAS FAIAL E TERCEIRA, AÇORES*

Dissertation submitted to the University of the Azores for award of  
degree of Doctor of Philosophy in Geology, speciality in Volcanology

*Dissertação apresentada à Universidade dos Açores para a obtenção do  
grau de Doutor no Ramo de Geologia, especialidade de Vulcanologia*

Supervisor/*Orientador*: Doutor José Pacheco

Co-supervisor/*Co-orientador*: Professor Stephen Self



UNIVERSIDADE DOS AÇORES  
DEPARTAMENTO DE GEOCIÊNCIAS  
2015

This work was financially supported by the Fundo Regional para a Ciência e Tecnologia by a PhD grant (M3.1.2/F/022/2007), on the scope of the Plano Integrado para a Ciência e Tecnologia (PICT) of the Azores Regional Government.

*Este trabalho teve o apoio financeiro do Fundo Regional para a Ciência e Tecnologia através de uma bolsa de Doutoramento (M3.1.2/F/022/2007), no âmbito do Plano Integrado para a Ciência e Tecnologia (PICT) do Governo Regional dos Açores.*

To my family  
Carla, Diogo and Carolina,  
and to my parents and brother

## Table of Contents

List of Figures .....	VI
List of Tables .....	XVI
Acknowledgments .....	XVIII
Abstract .....	XIX
Resumo .....	XXI

### SECTION I. GENERAL INTRODUCTION

<b>Chapter 1. Introduction</b> .....	2
1.1. Foreword .....	2
1.2. Geological setting of the Azores .....	5
1.3. Occurrence of ignimbrites in the Azores islands .....	8
1.4. Thesis objectives .....	14
1.5. Studied volcanic deposits .....	15
1.6. Methods of study .....	16
<b>Chapter 2. Pyroclastic density currents and ignimbrites: a review</b> ...	17
2.1. Introduction .....	17
2.2. Origin of pyroclastic density currents .....	19
2.2.1. <i>Fountain collapses</i> .....	19
2.2.2. <i>Collapses from lava domes and flows</i> .....	23
2.2.3. <i>Lateral directed blasts</i> .....	24
2.3. Transport processes in pyroclastic density currents .....	27
2.3.1. <i>Support by fluid turbulence</i> .....	28
2.3.2. <i>Support by fluidization</i> .....	31
2.3.3. <i>Support by particle interactions</i> .....	35
2.4. Depositional processes in pyroclastic density currents .....	38
2.4.1. <i>En masse deposition</i> .....	38
2.4.2. <i>Progressive aggradation (the flow-boundary zone approach)</i> .....	39

2.4.3. <i>Stepwise aggradation in pulsating pyroclastic density currents</i> .....	46
2.5. <b>Pyroclastic density current deposits</b> .....	47
2.5.1. <i>Aspect ratio of ignimbrites</i> .....	50
2.5.2. <i>Welding in ignimbrites</i> .....	52

## SECTION II. CASE STUDIES

<b>Chapter 3. The ~1000 years BP explosive caldera-forming eruption of Caldeira Volcano (Faial, Azores): physical volcanology, geochemistry and eruptive dynamics</b> .....	56
3.1. <b>Introduction</b> .....	56
3.2. <b>Geological setting and evolution of Faial Island</b> .....	59
3.3. <b>Methodology</b> .....	63
3.3.1. <i>Field studies</i> .....	63
3.3.2. <i>Grain size, component and morphology analyses</i> .....	64
3.3.3. <i>Petrography, whole-rock geochemistry and mineral chemistry analyses</i> .....	66
3.4. <b>Stratigraphy of the C11 deposit</b> .....	67
3.4.1. <i>Member 1: Brejo</i> .....	69
3.4.2. <i>Member 2: Inverno</i> .....	76
3.4.3. <i>Member 3: Cedros</i> .....	81
3.5. <b>Physical parameters</b> .....	93
3.5.1. <i>Volume, VEI, erupted mass and magnitude</i> .....	93
3.5.2. <i>Column height, mass eruption rate and intensity</i> .....	95
3.6. <b>Petrography and geochemistry</b> .....	99
3.6.1. <i>Petrographic aspects and mineral chemistry</i> .....	99
3.6.2. <i>Whole-rock and glass geochemistry</i> .....	103
3.6.3. <i>Magmatic intensive parameters</i> .....	107
3.7. <b>Eruption history</b> .....	108
3.7.1. <i>Phase 1: Phreatomagmatic</i> .....	108
3.7.2. <i>Phase 2: Magmatic fall-dominated</i> .....	110
3.7.3. <i>Phase 3: Magmatic caldera-forming</i> .....	111

3.8. Discussion .....	113
3.8.1. <i>Phreatomagmatic activity</i> .....	114
3.8.2. <i>Caldera collapse and influence of tectonics</i> .....	115
3.8.3. <i>Magma mingling/mixing</i> .....	116
3.9. Conclusions .....	118

## Chapter 4. The Lajes-Angra Ignimbrite Formation (Terceira, Azores): eruption, depositional processes and aspect ratio

of peralkaline ignimbrites .....	120
4.1. Introduction .....	120
4.2. Geological setting and evolution of Terceira Island .....	123
4.3. Methodology .....	127
4.3.1. <i>Field studies</i> .....	127
4.3.2. <i>Petrography, whole-rock geochemistry and mineral chemistry analyses</i> .....	128
4.4. Overview of the Lajes-Angra Ignimbrite Formation .....	130
4.5. Lithofacies of the Lajes and Angra ignimbrites .....	135
4.5.1. <i>Massive lapilli-ash (mLA)</i> .....	135
4.5.2. <i>Eutaxitic massive lapilli-ash (emLA)</i> .....	137
4.5.3. <i>Diffuse-stratified lapilli-ash (dsLA)</i> .....	139
4.5.4. <i>Diffuse-bedded lapilli-ash (dbLA)</i> .....	141
4.5.5. <i>Massive lithic breccias (mlBr)</i> .....	142
4.5.6. <i>Massive ash (mA)</i> .....	144
4.5.7. <i>Crystal-rich (lithic-rich) ash (crA, lA)</i> .....	145
4.6. Ignimbrite architecture .....	147
4.6.1. <i>Vertical variations</i> .....	147
4.6.2. <i>Lateral variations</i> .....	151
4.7. Physical parameters .....	154
4.7.1. <i>Areal distribution and aspect ratio</i> .....	154
4.7.2. <i>Volume, VEI, erupted mass and magnitude</i> .....	157

<b>4.8. Petrography and mineral chemistry</b> .....	160
<b>4.8.1. Petrographic and textural aspects</b> .....	160
<b>4.8.2. Mineral assemblage and chemistry</b> .....	163
<b>4.9. Whole-rock and glass geochemistry</b> .....	167
<b>4.9.1. Major elements of whole-rock and groundmass glass composition</b> .....	169
<b>4.9.2. Trace elements of whole-rock samples</b> .....	171
<b>4.10. Discussion</b> .....	175
<b>4.10.1. Magmatic intensive parameters</b> .....	176
<b>4.10.2. Magma reservoir processes</b> .....	177
<b>4.10.3. Eruption style and interaction with palaeotopography</b> .....	181
<b>4.11. Conclusions</b> .....	184

### SECTION III. FINAL REMARKS

<b>Chapter 5. Spin-off studies</b> .....	187
<b>5.1. Foreword</b> .....	187
<b>5.2. Paleomagnetic determination of emplacement temperatures of pyroclastic density currents from the ~1000 years BP eruption of Caldeira Volcano (Faial, Azores)</b> .....	188
<b>5.3. Magmatic processes revealed by textural and compositional features of anorthoclase phenocrysts from the Lajes Ignimbrite (Terceira, Azores)</b> .....	192
<b>Chapter 6. Main conclusions</b> .....	197
<b>References</b> .....	201

### APPENDICES

<b>Appendix A.1. Location of stratigraphic sections on Faial Island</b> .....	A1
<b>Appendix A.2. Location of C11 samples and analytical methods</b> .....	A6
<b>Appendix A.3. Whole-rock major element chemical analyses of C11 products</b> ..	A9
<b>Appendix A.4. Whole-rock trace element chemical analyses of C11 products</b> ....	A10

<b>Appendix A.5. Location of stratigraphic sections on Terceira Island .....</b>	<b>A12</b>
<b>Appendix A.6. Location of LAI samples .....</b>	<b>A15</b>
<b>Appendix A.7. Whole-rock major element chemical analyses of LAI products ..</b>	<b>A16</b>
<b>Appendix A.8. Whole-rock trace element chemical analyses of LAI products ....</b>	<b>A17</b>

## List of Figures

### Chapter 1.

<b>Figure 1.1.</b> Geological setting of the Azores (simplified from Lourenço et al., 1998; Vogt and Jung, 2004; Beier et al., 2008; Georgen and Sankar, 2010). MAR – Mid-Atlantic Ridge; TR – Terceira Rift ss; EAFZ – East Azores Fracture Zone; GF – GLORIA Fault. ....	5
<b>Figure 1.2.</b> Outcrop of the Lajes Ignimbrite west of Lajes village (type location; scale is 1 m). ....	11
<b>Figure 1.3.</b> Outcrop of the (Cedros) ignimbrite of C11 south of Cedros village (scale is 1 m). ....	12

### Chapter 2.

<b>Figure 2.1.</b> Different types of eruptive column regimes: (a) Convective column. (b) Transitional column. (c) Fountain collapse with formation of PDCs (adapted from Neri et al., 2002). ....	18
<b>Figure 2.2.</b> Fountain collapse during the AD 1984 eruption of Mayon Volcano, in the Philippines (photo by C. Newhall and sketch from Branney and Kokelaar, 2002). ....	20
<b>Figure 2.3.</b> Different types of fountain collapses: (a) Discrete collapse from a convective eruptive column producing highly unsteady PDCs. (b) Prolonged pyroclastic fountaining from an established eruptive column forming sustained quasi-steady PDCs. (c) Continuous low pyroclastic fountaining generating sustained quasi-steady PDCs (modified from Branney and Kokelaar, 2002). ....	22
<b>Figure 2.4.</b> Lava dome collapse during the AD 2010 eruption of Merapi Volcano, in Indonesia (photo by A. Prasetyo and sketch from Branney and Kokelaar, 2002). ....	23
<b>Figure 2.5.</b> Lateral directed blast during the AD 1980 eruption of Mt. St. Helens, in the United States (photo by G. Rosenquist and sketch from Branney and Kokelaar, 2002). ....	25
<b>Figure 2.6.</b> Two mechanisms of fluid support acting on particles with different shapes. On top, the aerofoil effect is a lift component transmitted to a particle when a horizontal fluid flow acts on the inclined surface. At the bottom, the Robins effect of a saltating particle that tends to rotate around axes transverse to the fluid flow (Branney and Kokelaar, 2002). ....	28

<b>Figure 2.7.</b> Vertical segregation of particles within turbulent currents, according to different transport mechanisms. The fraction of particles supported by fluid turbulence, the wash load, is distributed throughout the current. A second fraction of particles is intermittently supported by fluid turbulence and frequently returns to the substrate surface occurs in the lower part of the current, the saltation zone. A third fraction of particles is transported by traction along the surface of the substrate (after Branney and Kokelaar, 2002). .....	29
<b>Figure 2.8.</b> General scheme of a fluidized PDC, where clasts are supported by the upward flux of escaping gas ( $\rho$ – density; from Sulpizio and Dellino, 2008). .....	32
<b>Figure 2.9.</b> Different types of fluidization according to Branney and Kokelaar (2002). (a) Stationary fluidization (particulate vs. aggregative). (b) Flow fluidization. (c) Bulk self-fluidization. (d) Grain self-fluidization. (e) Sedimentation fluidization. ....	33
<b>Figure 2.10.</b> General scheme of a PDC dominated by granular flow regime, where kinetic sieving promotes the migration of small clasts to the base of the current and the apparent upward migration of coarser clasts (Sulpizio and Dellino, 2008). .....	36
<b>Figure 2.11.</b> Conceptual models of four end-member types of flow-boundary zone in steady currents, with schematic concentration, $C$ , and velocity, $u$ , profiles: (a) Location of the flow-boundary zone between the lowermost part of the current and the uppermost part of the aggrading deposit. (b) Direct fallout-dominated flow-boundary zone. (c) Traction-dominated flow-boundary zone. (d) Granular flow-dominated flow-boundary zone. (e) Fluid escape-dominated flow-boundary zone (Branney and Kokelaar, 2002). .....	41
<b>Figure 2.12.</b> The cube shows the conceptualization of the gradations between the four types of flow-boundary zone, according to variations of the three conditions represented by the axes: clast concentration, shear rate and rate of deposition (Branney and Kokelaar, 2002). .....	45
<b>Figure 2.13.</b> Examples of the two main types of PDC deposits from Tenerife (Canary Islands). (a) Massive PDC deposit (ignimbrite). (b) Stratified PDC deposit (pyroclastic surge deposit). .....	48

<b>Figure 2.14.</b> Cartoon illustrating the variation of lithofacies formed during deposition of the same PDC. The deposition of massive lithofacies in proximal regions, from a fluid escape-dominated flow-boundary zone, gradually changes to cross-stratified lithofacies, from traction-dominated flow-boundary zone, and to generally massive lithofacies with weak stratification in distal areas, from a flow-boundary zone with an important direct fallout component (simplified from Brown et al., 2007). .....	49
<b>Figure 2.15.</b> Schematic view of (a) a high-aspect ratio ignimbrite and (b) a low-aspect ratio ignimbrite. F – Extent of PDC deposits; S – Seard zone (pyroclastic surge); VP – Valley pond ignimbrite deposit; V – veneer deposit; G – Fines-depleted deposits underlying normal flow material (from Walker, 1983). .....	51
<b>Figure 2.16.</b> The welding grade continuum (Branney and Kokelaar, 1992). .....	54
 <b>Chapter 3.</b>	
<b>Figure 3.1.</b> (a) Simplified geological map of Faial Island (modified from Serralheiro et al., 1989); UTM coordinates, zone 26S. (b) Stratigraphic scheme and reconstruction of the different phases of evolution of Faial (adapted from Pacheco, 2001). In the Cedros Volcanic Complex Upper Group scheme the thickness, not to scale, shows the relative volumetric expression among deposits. ....	60
<b>Figure 3.2.</b> Map of the minimum extent of the C11 deposit on land, including fall and ignimbrite deposits, and documented stratigraphic sections (white circles). Main locality names referred throughout the text are shown; UTM coordinates, zone 26S. ....	64
<b>Figure 3.3.</b> Composite stratigraphic section of the C11 pyroclastic succession with reference to the members and corresponding eruptive phases. ....	68
<b>Figure 3.4.</b> Representative stratigraphic sections of Brejo Member showing lateral thickness variation. M1 – Brejo Member; M2 – Inverno Member; M3 – Cedros Member. ....	70

<b>Figure 3.5.</b> Deposits from Brejo Member at different stratigraphic sections (see Fig. 3.4 for location and lithofacies key). (a) Sequence of massive fine-grained ash beds and subordinate coarse-grained ash beds (section FAYL126; scale is 20 cm). (b) Sequence of massive coarse-grained ash beds with a massive pumice lapilli bed (section FAYL90; scale is 40 cm). (c) Stratified ash with local thickness variation in a sequence of parallel-bedded ash beds (section FAYL124; scale is 20 cm). (d) Accretionary lapilli and branch mould in a fine-grained ash bed (section FAYL123; pen for scale). M2 – Inverno Member. ....	71
<b>Figure 3.6.</b> SEM images of representative morphologies of juvenile ash particles. (a) Dense blocky clast with adherent fine-ash particles (sample FAYS103-1). (b) Subrounded clast with moss-like morphology (sample FAYS103-1). (c) Fused-shaped poorly vesiculated clast with adherent fine-ash particles (sample FAYS123-1). (d) Vesicular clast with thick walls cut by planar surfaces (sample FAYS123-3). ....	72
<b>Figure 3.7.</b> Typical stratigraphic section of Brejo Member along Alto do Brejo road (section FAYL123; see Fig. 3.4 for location and lithofacies key). Grain size histograms of selected beds are shown. ....	73
<b>Figure 3.8.</b> Isopach map of the Brejo Member ash layers sequence; UTM coordinates, zone 26S. ....	74
<b>Figure 3.9.</b> Diagram of sorting ( $\sigma\phi$ ) versus mean diameter ( $Md\phi$ ) for the ash beds from Brejo Member, with fall and flow contours defined by Walker (1971). ....	75
<b>Figure 3.10.</b> Representative stratigraphic sections of Inverno Member showing lateral thickness variation. M1 – Brejo Member; M2 – Inverno Member; 2A – Bed 2A; 2B – Bed 2B; M3 – Cedros Member. ....	77
<b>Figure 3.11.</b> Features of the Inverno Member at stratigraphic section FAYL145 (see Fig. 3.10 for location and lithofacies key). (a) Beds 2A and 2B lithofacies (scale is 20 cm. M1 – Brejo Member; M3 – Cedros Member). (b) Framework-supported coarse-grained pumice and lithic lapilli. (c) Pumice block with impact fractures. (d) From left to right, light-coloured, banded and dark-grey pumice clasts. ....	78
<b>Figure 3.12.</b> Typical stratigraphic section of Inverno Member along Alto do Inverno road (FAYL73; see Fig. 3.10 for location and lithofacies key). Grain size and component histogram is also shown. ...	79

<b>Figure 3.13.</b> Isopach map of the Inverno Member coarse pumice fall deposit; UTM coordinates, zone 26S. ....	80
<b>Figure 3.14.</b> Representative stratigraphic sections of Cedros Member showing thickness and lithofacies variations. M1 – Brejo Member; M2 – Inverno Member; M3 – Cedros Member. ....	82
<b>Figure 3.15.</b> Deposits from Cedros Member at different stratigraphic sections (see Fig. 3.14 for location and lithofacies key; scale is 1m). (a) Massive lapilli-ash with pumice-rich horizon and standing charred tree trunk (section FAYL12). (b) Lithic-rich diffuse-bedded lapilli-ash grading upward into massive lapilli-ash (section FAYL69). (c) Pumice-rich massive lapilli-ash grading upward to diffuse-stratified lapilli-ash and back to massive lapilli-ash (section FAYL150). (d) Massive lithic breccia (section FAYL32). ....	84
<b>Figure 3.16.</b> Typical stratigraphic sections of Cedros Member at Cancelas and Canada Larga quarries (FAYL12 and FAYL46, respectively; see Fig. 3.14 for location and lithofacies key). Grain size and component histograms are also shown. ....	85
<b>Figure 3.17.</b> Distribution map of the Cedros Member PDC associated deposits; UTM coordinates, zone 26S. ....	89
<b>Figure 3.18.</b> Diagram of log of thickness vs. square root of area for Brejo and Inverno members. The calculated volumes for single segments are reported. White diamonds – Brejo data; Grey circles – Inverno data. ....	94
<b>Figure 3.19.</b> Isopleth maps of the Inverno Member. (a) Lithic isopleths. (b) Pumice isopleths; UTM coordinates, zone 26S. ....	96
<b>Figure 3.20.</b> (a) Crosswind range vs. downwind range diagram for 6.4 cm clast diameter with 2500 kg/m <sup>3</sup> of density (Carey and Sparks, 1986) used to estimate column height and wind speeds for the magmatic fall-dominated phase of the eruption. (b) Half-distance ratio (bc/bt) vs. thickness half-distance diagram (bt), where bc is the clast half distance and Ht is the total column height (Pyle, 1989), used to classify eruptive style of the Inverno Member. Grey circle – Lithics; White circle – Pumices. ....	97

<b>Figure 3.21.</b> Microphotographs of pumice from the C11 deposit. (a) Light-coloured pumice with large subcircular vesicles and subhedral plagioclase phenocryst – Pl. (b) Dark-grey pumice with small irregularly-shaped vesicles and euhedral plagioclase phenocryst – Pl. (c) Plagioclase phenocryst – Pl, with sieve texture and microphenocrysts of clinopyroxene. (d) Euhedral olvine xenocryst – Ol. (e) Euhedral amphibole phenocryst – Amp. (f) Partially resorbed biotite phenocryst – Bt. ....	100
<b>Figure 3.22.</b> Total alkalis versus silica (TAS) diagram (Le Bas et al., 1986) for the classification of C11 pumice and groundmass glass. ....	104
<b>Figure 3.23.</b> Variation diagrams for major elements (wt%) versus SiO <sub>2</sub> (wt%) for C11 whole-rock pumice and groundmass glass. ....	105
<b>Figure 3.24.</b> Primordial mantle-normalised multi-element diagram (McDonough and Sun, 1995) for C11 pumices. Six samples, including light-coloured, dark-grey and banded clasts, are plotted in the diagram; shaded area includes pumices from the Cedros Volcanic Complex Upper Group (Zanon et al., 2013). ....	106
<b>Figure 3.25.</b> Sketch showing a summary of the eruptive phases. (a) Phreatomagmatic phase. (b) Magmatic fall-dominated phase. (c) Magmatic caldera-forming phase. Eruptive columns and PDCs are not to scale. ....	109
 <b>Chapter 4.</b>	
<b>Figure 4.1.</b> (a) Simplified geological map of Terceira Island (modified from Madeira, 2005); UTM coordinates, zone 26S. (b) Stratigraphic scheme and reconstruction of the different phases of evolution of Terceira (ages from Calvert et al., 2006; Gertisser et al., 2010; Hildenbrand et al., 2014) LAI – Lajes-Angra Ignimbrite Formation. ....	124
<b>Figure 4.2.</b> Outcropping areas of the Lajes-Angra Ignimbrite Formation and documented stratigraphic sections (white circles). Locality names referred throughout the text are shown; UTM coordinates, zone 26S. ....	127
<b>Figure 4.3.</b> Correlation of ignimbrite formations on Terceira, showing average ages and maximum errors for formations found on the north and south coasts and in the interior of the island. Ignimbrite members are given in parenthesis; see text for abbreviations (adapted from Gertisser et al., 2010). ...	130

<b>Figure 4.4.</b> Generalized stratigraphic sections of the (a) Lajes Ignimbrite and the (b) Angra Ignimbrite, with reference to the main lithofacies and interpretation. ....	133
<b>Figure 4.5.</b> Radiocarbon ages of the Lajes-Angra Ignimbrite Formation. White circles – Lajes Ignimbrite; Grey circles – Angra Ignimbrite. Ages from Self (1974, 1976) <sup>a</sup> were obtained by Shotton and Williams (1973) and Shotton et al. (1974). ....	134
<b>Figure 4.6.</b> Typical aspect of the massive lapilli-ash (mLA) deposits from (a) Lajes Ignimbrite (section TERL2; scale is 1 m) and (b) Angra Ignimbrite (section TERL63; circle encloses 1 m scale). (c) Fine-grained massive lapilli-ash from Lajes Ignimbrite (section TERL23; pen for scale). (d) Coarse-clast bearing massive lapilli-ash with scoriae to dense vitrophyres, from the upper part of Lajes Ignimbrite (section TERL62; scale is 20 cm). (e) From left to right: light-grey pumice, coarsely porphyritic dark-grey scoriae and coarsely porphyritic black dense vitrophyric clasts. ....	136
<b>Figure 4.7.</b> Eutaxitic massive lapilli-ash (emLA) deposits from Lajes Ignimbrite. (a) Gradual transition from densely welded base to poorly welded upper part (section TERL61; scale is 20 cm). (b) Detail of the matrix with eutaxitic texture, including glassy lapilli-size fiamme (section TERL61; pen for scale). (c) Poorly welded deposit with coexisting flatten (oblate clasts) and subrounded scoriaceous clasts (section TERL2; scale is 20 cm). ....	138
<b>Figure 4.8.</b> (a) Diffuse-stratified lapilli-ash (dsLA) deposits from Lajes Ignimbrite (section TERL59; scale is 20 cm). (b) Diffuse-stratified lapilli-ash with lateral thickness variation and discontinuous stratification (section TERL10; scale is 40 cm), overlaid by lithic-rich massive lapilli-ash (lmLA). ..	140
<b>Figure 4.9.</b> Diffuse-bedded lapilli-ash (dbLA) deposits from Lajes Ignimbrite (section TERL59; scale is 1 m), overlaying diffuse-stratified lapilli-ash (dsLA). ....	141
<b>Figure 4.10.</b> (a) Massive lithic breccia (mlBr) from Lajes Ignimbrite (section TERL36; scale is 1 m). (b) Detail of matrix-supported massive lithic breccia, with various types of lithic clasts and a dense vitrophyric juvenile clast (section TERL39; pen for scale). ....	143
<b>Figure 4.11.</b> (a) Massive ash (mA) at the base of Lajes Ignimbrite, grading from light-coloured to dark-grey (section TERL20; pen for scale). (b) Detail of the massive ash with scattered feldspar crystals (section TERL20). (c) Massive ash with carbonized wood fragments (section TERL14). ....	144

<b>Figure 4.12.</b> (a) Fines-poor crystal-rich ash (crA) at the base of Lajes Ignimbrite (section TERL18). (b) Detail of the enrichment in lithics (LA) (section TERL37; pens for scale). .....	145
<b>Figure 4.13.</b> Representative stratigraphic sections of the Lajes Ignimbrite along the north coastal area of Terceira. ....	148
<b>Figure 4.14.</b> Representative stratigraphic sections of the Lajes and Angra ignimbrites along the south coastal area of Terceira. LI – Lajes Ignimbrite; AI – Angra Ignimbrite. ....	149
<b>Figure 4.15.</b> View of the cliffs along the north coast of Terceira showing the Lajes Ignimbrite overlaying a sequence of older pyroclastic formations. ....	152
<b>Figure 4.16.</b> Distribution map of Lajes Ignimbrite. Arrows indicate the main flow paths; UTM coordinates, zone 26S. ....	155
<b>Figure 4.17.</b> Distribution map of Angra Ignimbrite. Arrows indicate the main flow paths; UTM coordinates, zone 26S. ....	156
<b>Figure 4.18.</b> Microphotographs of representative textures of the LAI juvenile clasts. (a) Light-coloured pumice with large subcircular vesicles. (b) Microvesicular scoria with subcircular to slightly elongated vesicles and an alkali feldspar phenocryst. (c) Scoria with strongly stretched and coalescent vesicles in brown glassy groundmass, note the euhedral Fe-Ti oxide microphenocryst. (d) Contrast between bands of cryptocrystalline devitrified glass and fresh microlite-free glass. (e) Vitrophyre with brown glassy groundmass with collapsed vesicles and dispersed tabular alkali feldspar microphenocryst. (f) Cluster of spherulites growing around vesicles and an euhedral clinopyroxene microphenocryst. ....	162
<b>Figure 4.19.</b> Microphotographs of representative features of the LAI mineral phases. (a) Euhedral alkali feldspar phenocryst. (b) Alkali feldspar phenocryst with embayment structures. (c) Alkali feldspar phenocryst with partially resorbed core filled by vesicular glassy pockets. (d) Fractured alkali feldspar phenocryst. (e) Subhedral clinopyroxene phenocryst with Fe-Ti oxide inclusions. (f) Olivine phenocrysts with reaction rims and inclusions of Fe-Ti oxides and small acicular apatite. ....	165

<b>Figure 4.20.</b> Classification diagrams of mineral phases of the LAI. (a) Alkali feldspar compositions plotted into the An-Ab-Or diagram. (b) Clinopyroxene compositions plotted into the Wo-En-Fs quadrilateral diagram (Morimoto, 1989). (c) Fe-Ti oxide compositions plotted into the $TiO_2$ -FeO- $Fe_2O_3$ diagram. ....	166
<b>Figure 4.21.</b> (a) Total alkalis versus silica (TAS) diagram (Le Bas et al., 1986) for the classification of LAI whole-rock and groundmass glass. (b) $FeO_t$ versus $Al_2O_3$ diagram (Macdonald, 1974) for the classification of LAI peralkaline rocks and groundmass glasses. ....	168
<b>Figure 4.22.</b> Variation diagrams for major elements (wt%) versus $SiO_2$ (wt%) for LAI whole-rock and groundmass glass. All analyses are normalised to 100 wt% on a volatile-free basis. ....	170
<b>Figure 4.23.</b> Variation diagrams of sulphur and chlorine (wt%) versus $SiO_2$ (wt%) for LAI groundmass glasses. Symbols as in Fig. 4.22. ....	171
<b>Figure 4.24.</b> Variation diagrams for trace elements (ppm) versus $SiO_2$ (wt%) for LAI whole-rock. Symbols as in Fig. 4.22. ....	172
<b>Figure 4.25.</b> (a) Chondrite-normalised Rare Earth Element (REE) diagram Sun and McDonough (1989) for LAI whole-rock. (b) Primordial mantle-normalised multi-element diagram (McDonough and Sun, 1995) for LAI whole-rock. ....	173
<b>Figure 4.26.</b> Nb and Ba (ppm) versus Zr (ppm) diagrams showing the degree of evolution of LAI whole-rock samples. The sample TERS prefix was omitted for simplification purposes. Symbols as in Fig. 4.22. ....	173
<b>Figure 4.27.</b> Conceptual model of the LAI magma reservoir, showing different magmatic and eruptive processes. ....	178
 <b>Chapter 5.</b>	
<b>Figure 5.1.</b> Paleomagnetic data of a representative sample (FAYL72-06) from the north flank of Caldeira Volcano (distal location). Intensity decay diagram, equal area stereonet of the mean remanence directions and vector plot showing one stable component of magnetization. ....	188

<b>Figure 5.2.</b> Paleomagnetic data of representative samples (FAYL12-03 and FAYL12-06) from the Pedro Miguel Graben (northern flow path). Intensity decay diagram, equal area stereonet of the mean remanence directions and vector plot showing (a) one stable component of magnetization and (b) two components: a low-temperature (LT) magnetic component and a high-temperature (HT) magnetic component. ....	189
<b>Figure 5.3.</b> Paleomagnetic data of a representative sample (FAYL80-06) from the Pedro Miguel Graben (southern flow path). Intensity decay diagram, equal area stereonet of the mean remanence directions and vector plot showing two magnetic components: low-temperature (LT) and high-temperature (HT). ....	190
<b>Figure 5.4.</b> Distribution of the Cedros ignimbrite and emplacement temperatures of PDCs generated during the ~1000 years BP eruption of Caldeira Volcano. ....	191
<b>Figure 5.5.</b> Representative cathodoluminescence images of Type 1 anorthoclase phenocrysts. Arrows in (a) indicate the occurrence of wavy surfaces in the outer cores of the crystals and in (c) the rounded profile of zonation. White circles correspond to analyses spots. ....	193
<b>Figure 5.6.</b> Selected images of Type 2 anorthoclase phenocrysts: (a) under stereomicroscope, (b) at backscattered electron mode at scanning electron microscope and (c to f) at cathodoluminescence imaging. Arrows in (b) indicate corrosion gulfs with crypto crystalline rims and vesicular glass. White circles correspond to analyses spots. ....	194
<b>Figure 5.7.</b> Variation of Ba, Rb, Sr, La, Eu contents in Type 1 (open symbols) and Type 2 (closed symbols) anorthoclase with respect to An mol%. Vertical lines are the lower and upper limits of the field where the two types of crystals have similar composition. ....	195
<b>Figure 5.8.</b> Schematic transect of the magma reservoir beneath Pico Alto Volcano, with references to the different processes occurring prior to the eruption of the Lajes Ignimbrite. ....	196

## List of Tables

### Chapter 3.

<b>Table 3.1.</b> Statistical parameters of grain size distributions (Inman, 1952) of representative samples from beds of Brejo Member (Md $\phi$ – Mean diameter; $\sigma\phi$ – Graphic standard deviation or Sorting; $\alpha\phi$ – First order skewness; see Fig. 3.4 for location and lithofacies key). .....	74
<b>Table 3.2.</b> Maximum clast size at selected locations of Inverno Member (the maximum size of pumice and lithic clasts were determined by the average length of the major axis of the three largest clasts; see Fig. 3.10 for location). .....	79
<b>Table 3.3.</b> Statistical parameters of grain size distributions (Inman, 1952; Folk and Ward, 1957) of representative samples from Cedros Member (Md $\phi$ – Mean diameter; $\sigma\phi$ – Graphic standard deviation or Sorting; Mz – Graphic mean; $\sigma 1$ – Inclusive graphic standard deviation or Sorting; see Fig. 3.14 for location and lithofacies key). .....	83
<b>Table 3.4.</b> Summary of the physical parameters of the deposits of the ~1000 years BP eruption. ....	95
<b>Table 3.5.</b> Brief macroscopic description of the samples and correspondence with the members (PO – Petrographic observations; EMPA – Electron microprobe analyses; WRA – Whole-rock analyses; see Fig. 3.4, 3.10 and 3.14 for location and lithofacies key). .....	99
<b>Table 3.6.</b> Average chemical composition of mineral phases from C11 juvenile products. All values in wt%. (Pl – Plagioclase; Af – Alkali Feldspars; Ol – Olivine; Amp – Amphibole; Bt – Biotite; Cpx – Clinopyroxene; Mt – Magnetite; Ilm – Ilmenite; Ap – Apatite; No. – Number of analyses). .....	102
<b>Table 3.7.</b> Average C11 pumice whole-rock and groundmass glass composition. All values in wt%. (No. – Number of analyses). .....	103

### Chapter 4.

<b>Table 4.1.</b> Radiocarbon and calibrated ages of the Lajes-Angra Ignimbrite Formation. ....	134
<b>Table 4.2.</b> Summary of the physical parameters of the Lajes-Angra Ignimbrite Formation. ....	159

---

<b>Table 4.3.</b> Brief macroscopic description of the samples, with correspondence to the ignimbrites and lithofacies (WRA – Whole-rock analyses; PO – Petrographic observations; EMPA – Electron microprobe analyses; see Fig. 4.13 and 4.14 for location and lithofacies key as in previous sections).	160
<b>Table 4.4.</b> Average chemical composition of mineral phases from the LAI. All values in wt%. (Af – Alkali Feldspar; Cpx – Clinopyroxene; Ol – Olivine; Mt – Magnetite; Ilm – Ilmenite; Ap – Apatite; No. – Number of analyses).	163
<b>Table 4.5.</b> Average whole-rock and groundmass glass composition of Lajes and Angra ignimbrites. Analyses are normalised to 100 wt% on a volatile-free basis. All values in wt% (No. – Number of analyses; PI – Peralkalinity index).	167

## **Acknowledgments**

This work would not have been possible without the help, contribution and support of many people and institutions. I would like to take this opportunity to acknowledge all of them.

I want to express my appreciation to the following institutions:

The University of the Azores and the Department of Geosciences, in particular to the directors, professors and staff who accompanied me since the start of my academic life.

The Centre of Volcanology and Geological Risk Assessment (CVARG) and the Centre of Information and Seismovolcanic Surveillance of the Azores (CIVISA) for the financial support, the facilities granted and especially for the ever present generosity that allowed the development of this work.

I would like to thank my supervisors Doctor José Pacheco and Professor Stephen Self for their advice, discussions and reviews, but mainly for all the patience revealed.

Special thanks to all my friends, colleagues and co-workers who somehow helped me through these long years.

In particular, Ana Mendes, Vittorio Zanon and Max Porreca are thanked for their help in the field and in the laboratory, and for their stimulating and constructive comments during different phases of the work which significantly improved this thesis.

Finally, I would like to thank my parents and brother for the constant support, encouragement and for believing in me until the end. Most importantly, thanks to my wife Carla and my beautiful Carolina and Diogo for the all the love.

Thank you!

## Abstract

The Azores archipelago has an extensive stratigraphic record of pyroclastic density current-forming eruptions. Such eruptions typically occur on active central volcanoes and are associated with paroxysmal events of caldera formation. This work focuses on two contrasting pyroclastic density current-forming episodes on the islands of Faial and Terceira, in order to obtain a comprehensive understanding of the diversity of eruptive styles that can produce ignimbrites.

The ~1000 years BP eruption of Caldeira Volcano (Faial Island) was the last major pyroclastic density current-forming eruption associated with a caldera collapse in the Azores. It produced a complex pyroclastic succession, known as the C11 deposit, which is divided into three members with distinct lithofacies: a lower sequence of ash layers (Brejo Member) found in the NW sector of Faial, an intermediate pumice fall deposit (Inverno Member) restricted to the north flank of the volcano and an upper ignimbrite and associated lithic breccias (Cedros Member) exposed along the north and east flanks. These record three phases of the eruption with different eruptive styles. The eruption started with a phreatomagmatic phase that produced ash fallout and fully dilute density currents, followed by a magmatic fall-dominated phase with the establishment of a sub-Plinian column (up to 14 km high) and culminated with a climatic caldera-forming phase that generated extensive pyroclastic density currents and led to caldera collapse. This marked the first stage of formation of an incremental caldera at the volcano.

Overall, a minimum bulk volume of at least 0.18 km<sup>3</sup> was estimated for this caldera-forming eruption, although a significant portion of material was deposited offshore. The juvenile products (light-coloured, dark-grey and banded pumices) have a homogeneous trachytic composition (59 wt% SiO<sub>2</sub>). However, petrographic and groundmass glass analyses indicate that the C11 magma resulted from the mingling/mixing between two trachytic batches of magma with different degrees of evolution. The emplacement temperatures of pyroclastic density currents on the north flank of the volcano were estimated at >550-560 °C, while along Pedro Miguel Graben were at lower temperatures of 300-560 °C.

The Lajes-Angra Ignimbrite Formation (Terceira Island) is one of the largest and best exposed ignimbrite formations in the Azores. It is comprised of two members with ~21 ka: the Lajes and the Angra ignimbrites of Pico Alto Volcano. The Lajes Ignimbrite (0.59 km<sup>3</sup> bulk volume) is a low-aspect ratio ignimbrite with vertical lithofacies variations marked by an upward coarsening of the sequence. It has an extensive distribution across much of the island, showing lateral thickness and lithofacies variations. The Angra Ignimbrite (0.08 km<sup>3</sup> bulk volume) is a thick monotonous ignimbrite mostly restricted to one valley on the south part of the island.

These ignimbrites record two closely spaced in time pyroclastic density current-forming events of Pico Alto. The first corresponds to the Angra Ignimbrite eruption and was characterized by a short-lived pyroclastic fountain that generated a small volume sustained pyroclastic density current, almost totally channelled along a valley. The second eruptive event is recorded by the Lajes Ignimbrite and was marked by vigorous and prolonged pyroclastic fountaining that formed a sustained quasi-steady pyroclastic density current. It spread radially from Pico Alto caldera to the north and south coasts. The low-aspect ratio of this ignimbrite resulted from the widespread deposition of a relatively low velocity pyroclastic density current over the smooth palaeotopography of Terceira.

The juvenile clasts of the two ignimbrites include pumices and porphyritic scoriae (dense vitrophyres are only found on Lajes Ignimbrite) with similar peralkaline comenditic trachyte composition (65-66 wt% SiO<sub>2</sub>) and mineral assemblage. Despite of relatively homogenous major element compositions, disequilibrium textures in crystals (especially alkali feldspars) and trace element variability suggest that the magma reservoir was compositionally zoned before the eruption of the ignimbrites. The zonation seems to have been disrupted by pre- and syn-eruptive mixing/mingling of magmas. The presence of two different types of anorthoclase phenocrysts in the Lajes Ignimbrite confirmed the occurrence of crystal convection in the reservoir and interaction with a hotter magma.

## Resumo

O arquipélago dos Açores possui um extenso registo estratigráfico de erupções formadoras de produtos piroclásticos de fluxo. Estas erupções ocorrem normalmente nos vulcões centrais activos e estão relacionadas com eventos paroxismais de formação de caldeira. O presente trabalho incide sobre dois destes episódios que originaram produtos piroclásticos de fluxo nas ilhas do Faial e da Terceira, tendo como objectivo obter uma melhor compreensão acerca da diversidade de estilos eruptivos que podem produzir ignimbritos.

A erupção de há ~1000 anos BP do Vulcão da Caldeira (Ilha do Faial) foi a última grande erupção formadora de produtos piroclásticos de fluxo associada a um colapso de caldeira nos Açores. Esta erupção produziu uma sequência piroclástica complexa, denominada como depósito C11, que se encontra dividida em três membros com litofácies distintas: a parte inferior corresponde a uma sequência de níveis de cinzas (Membro do Brejo) localizada no sector NW do Faial, a intermédia a um depósito de pedra pomes de queda (Membro do Inverno) limitado ao flanco norte do vulcão e a parte superior a um ignimbrito com brechas associadas (Membro dos Cedros) que aflora ao longo dos flancos norte e leste. Estes membros resultaram de três fases da erupção com diferentes estilos eruptivos. A erupção começou com uma fase freatomagmática que originou queda de cinzas e produtos de fluxo diluídos, seguiu-se uma fase magmática dominada por produtos de queda resultantes de uma coluna eruptiva sub-Pliniana (com cerca de 14 km de altura) e culminou com uma fase paroxismal de formação de caldeira que gerou produtos piroclásticos de fluxo e levou ao colapso da caldeira. Esta correspondeu à primeira fase da formação de uma caldeira de incremento neste vulcão.

Um volume eruptivo mínimo de pelo menos  $0,18 \text{ km}^3$  foi estimado para esta erupção formadora de caldeira, embora uma importante porção de material tenha sido depositada ao largo da ilha. Os produtos juvenis (pedra pomes de cor clara, cinza-escuro e bandada) possuem uma composição traquítica homogénea (59 wt% de  $\text{SiO}_2$ ). Contudo, análises petrográficas e do vidro da massa de fundo indicam que o magma de C11 resultou da mistura entre dois corpos magmáticos de natureza traquítica com diferentes graus de evolução. As temperaturas de deposição dos produtos piroclásticos de fluxo no flanco

norte do vulcão foram estimadas em >550-560 °C, enquanto que no *Graben* de Pedro Miguel as temperaturas foram inferiores entre 300-560 °C.

A Formação Ignimbrítica Lajes-Angra (Ilha Terceira) corresponde a uma das maiores e melhor expostas formações ignimbrítica dos Açores. É composta por dois membros com ~21 mil anos: os ignimbritos das Lajes e de Angra do Vulcão do Pico Alto. O Ignimbrito das Lajes (com um volume eruptivo de 0,59 km<sup>3</sup>) é um ignimbrito de baixo coeficiente de aspecto que apresenta variações verticais de litofácies, caracterizadas por um aumento ascendente da granulometria da sequência. Este ignimbrito tem uma ampla dispersão por grande parte da ilha, apresentando variações laterais de espessura e de litofácies. O Ignimbrito de Angra (volume eruptivo de 0,08 km<sup>3</sup>) é um ignimbrito muito homogêneo que se encontra limitado a um vale na parte sul da ilha.

Estes ignimbritos resultam de dois eventos formadores de produtos piroclásticos de fluxo do Pico Alto próximos no tempo. O primeiro corresponde à erupção do Ignimbrito de Angra e foi caracterizado por uma fonte piroclástica de curta duração que gerou um fluxo piroclástico sustentado de pequeno volume, quase totalmente canalizado ao longo de um vale. O segundo evento eruptivo produziu o Ignimbrito das Lajes, tendo sido marcado por uma fonte piroclástica vigorosa e prolongada que originou um fluxo piroclástico sustentado *quasi*-estável. Este fluxo dispersou-se radialmente desde a caldeira do Pico Alto até às costas norte e sul da ilha. O baixo coeficiente de aspecto deste ignimbrito resultou essencialmente da extensa deposição de um fluxo piroclástico, de velocidade relativamente baixa, sobre a suave paleotopografia da Terceira.

Os clastos juvenis dos dois ignimbritos incluem pedra pomes e escórias porfiríticas (clastos vitrofíricos ocorrem apenas no Ignimbrito das Lajes) com composição peralcalina semelhante, traquíticos comendíticos (65-66 wt% SiO<sub>2</sub>), e as mesmas fases minerais. Apesar das composições relativamente homogêneas em termos de elementos maiores, a presença de texturas de desequilíbrio em cristais (especialmente nos feldspatos alcalinos) e a variabilidade dos elementos em traço sugerem que o reservatório magmático era composicionalmente zonado antes da erupção dos ignimbritos. Este zoneamento parece ter sido estabilizado por processos de mistura pré- e sin-eruptiva de magmas. A presença de dois tipos de fenocristais de anortoclase no Ignimbrito das Lajes confirmou a ocorrência de convecção de cristais no reservatório e a interação com um magma mais quente.

## **SECTION I.**

### **GENERAL INTRODUCTION**

# Chapter 1.

## Introduction

### 1.1. Foreword

Volcanic eruptions are one of the most fascinating natural events on Earth. They are the surface expression of the planet's internal dynamics and usually occur along the margins of the lithospheric plates, in different geodynamic settings, where plates converge, diverge or sideslip one another. Intraplate volcanism also occurs in several places around the globe, away from plate margins, where is fed by deep magmatic plumes. The type of eruption strongly depends on the physical and chemical properties of the available magma, on the ascent path, through complex plumbing systems of fractures and conduits, and on the different surface environments that may or not contain water.

There is a remarkable variety of volcanic eruptions on Earth, ranging between two end-members according to their explosivity. Effusive eruptions occur when magma reaches the surface, essentially in a non-explosive manner, as a coherent fluid to form lava flows. By contrast, explosive eruptions result from the abrupt disruption of magma and consequent generation of fragments, which are ejected from the vent to form pyroclastic deposits.

Explosive volcanic eruptions are characterized by different eruptive styles and associated volcanic phenomena, including tephra fall, pyroclastic density currents (PDCs) and others. It is well known that explosive eruptions may have a significant impact on millions of people worldwide and on the global climate. Among the various volcanic phenomena, PDCs are the most destructive and lethal, having caused severe damage to buildings, infrastructures and agricultural lands, and several tens of thousands of deaths over the centuries.

Although direct observations of hazardous volcanic phenomena are infrequent and somewhat challenging, real-time observational and monitoring techniques have significantly improved the understanding of the emplacement dynamics of these volcanic products. However, there are numerous active volcanoes that did not erupt in historical times, but have a high eruptive potential. In these cases, the reconstruction of past explosive eruptions, based on fieldwork and analytical studies, is crucial for the proper assessment and mitigation of the volcanic hazards associated with future explosive events.

The work presented here focuses on the study of PDC-forming eruptions in the Azores archipelago. It documents two case studies: the ~1000 years BP explosive caldera-forming eruption on Faial Island and the Lajes-Angra Ignimbrite Formation on Terceira Island. In both cases, the eruption histories, transport and depositional processes are reconstructed mainly through physical volcanology-based studies, complemented with petrological and geochemical analysis. This thesis is intended to be the first comprehensive study on Azorean PDC-forming eruptions and a basis for comparison with past and current events worldwide.

The thesis is organized into three sections and six chapters:

The first section is composed of Chapters 1 and 2 and is intended to provide an overview of the work and of the main theoretical concepts. This first chapter includes a short review of the geological setting of the Azores archipelago and a brief description of the occurrence of ignimbrites and other PDC deposits on the islands of the Azores. The thesis objectives are outlined and the selected deposits and methodologies are presented.

Chapter 2 is a literature review on PDCs and ignimbrites. It discusses the various volcanic processes that can originate PDCs, the main processes of transport acting on density currents and the different conceptual models of deposition. The types of deposits formed by PDCs are discussed, as well as, common classification schemes of ignimbrites used during this work.

The second section of the thesis includes Chapters 3 and 4 that report two case studies of PDC-forming events in the Azores. These comprehensive studies document contrasting styles of eruptions that generated the largest ignimbrite sheets on the islands of Faial and Terceira.

Chapter 3 reports on the ~1000 years BP explosive caldera-forming eruption of Caldeira Volcano (Faial Island), the last major PDC-forming eruption recorded in the Azores archipelago. This work combines mapping and lithofacies analyses with the study of the grain size, componentry and morphological features of the erupted products. It is complemented by petrography, mineral and whole-rock geochemistry analyses of the juveniles. The new data allowed to reconstruct the eruption history and to shed light on eruptive and depositional processes occurring during the different phases of the eruption. Magma interaction processes are also briefly discussed.

Chapter 4 is dedicated to the study of the Lajes-Angra Ignimbrite Formation (~21 ka) on Terceira Island, one of the largest PDC-forming events recorded in the Azores. The Lajes and Angra ignimbrites are studied in parallel through a combination of lithofacies analyses, ignimbrite architecture and mapping, coupled with petrography, mineral chemistry and whole-rock geochemistry analyses of the juveniles. This work enabled to investigate crucial features of low-aspect ratio ignimbrites, including eruptive and depositional processes, and to reassess the common use of the aspect ratio as a measure of PDC dynamics. Particular attention was also given to pre- and syn-eruptive processes occurring in the magma reservoir.

The third section consists of final remarks and includes Chapters 5 and 6. Chapter 5 presents the summaries of two spin-off studies that arose during the development of the thesis and further contribute to improve the understanding of PDC-forming eruptions. One study is dedicated to the estimation of the emplacement temperatures of PDCs generated during the ~1000 years BP explosive eruption of Caldeira Volcano (Faial) through paleomagnetic methods. The other study looks into the magmatic processes associated with the eruption of the Lajes Ignimbrite (Terceira), mainly based on analyses of equilibrium and disequilibrium textures and compositional features of anorthoclase phenocrysts. Chapter 6 summarizes the main findings of this work.

## 1.2. Geological setting of the Azores

The Azores archipelago is located in the middle of the North Atlantic Ocean, between the latitudes 36°55' and 39°44' N and the longitudes 24°46' and 31°17' W, about 1300 km west of mainland Portugal. It is composed of nine islands distributed by three geographic groups: Ocidental (Flores and Corvo), Central (Faial, Pico, São Jorge, Graciosa and Terceira) and Oriental (São Miguel and Santa Maria). The islands are arranged diagonally along approximately 600 km in a NW-SE trend from Corvo to Santa Maria (Fig. 1.1). The Azores islands themselves are the emergent portions of large submarine volcanic edifices that rise from the oceanic Azores Plateau (e.g. Searle, 1980; Lourenço et al., 1998; Gente et al., 2003).

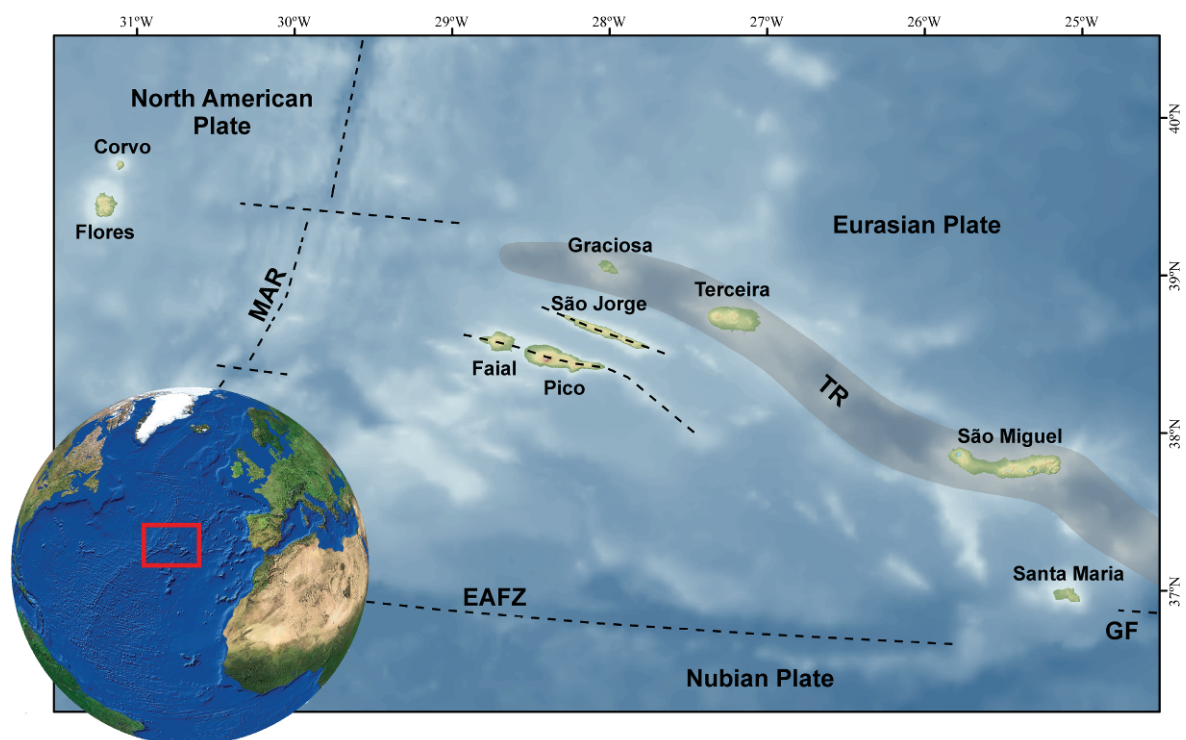


**Figure 1.1.** Geological setting of the Azores (simplified from Lourenço et al., 1998; Vogt and Jung, 2004; Beier et al., 2008; Georgen and Sankar, 2010). MAR – Mid-Atlantic Ridge; TR – Terceira Rift ss; EAFZ – East Azores Fracture Zone; GF – GLORIA Fault.

The unique setting in which the Azores archipelago stands, as result of the triple junction of the North American, Eurasian and Nubian lithospheric plates (Fig. 1.1), is prone to frequent moderate to low magnitude seismicity and volcanic activity. In this area of the North Atlantic Ocean, the plate boundaries of the Azores Triple Junction are marked by the presence of important structures, such as the Mid-Atlantic Ridge, the Terceira Rift, the East Azores Fracture Zone and the GLORIA Fault (e.g. Krause and Watkins, 1970; Searle, 1980; Madeira and Ribeiro, 1990; Miranda et al., 1991; Luis et al., 1994; Gente et al., 2003; Vogt and Jung, 2004; Fernandes et al., 2006; Dias et al., 2007).

The Mid-Atlantic Ridge clearly delimits the Eurasian and Nubian lithospheric plates to the east from the North-American plate to the west. In the Azores region, the Eurasian-Nubian boundary is complex and its precise kinematics is not yet fully understood. The westernmost segment of this plate boundary is generally known as the Terceira Rift and corresponds to the alignment of alternating basins and volcanic edifices (islands and seamounts) trending WNW-ESE. This area behaves as a right transtensional domain, reflecting simultaneously the hyper-slow oblique spreading rate of this plate boundary and the shear zone that accommodates the differential movement between the Eurasian and Nubian lithospheric plates (Krause and Watkins, 1970; Laughton and Whitmarsh, 1974; Searle, 1980; Madeira and Ribeiro, 1990; Madeira and Brum da Silveira, 2003; Vogt and Jung, 2004; Fernandes et al., 2006; Dias et al., 2007; Verzhbitsky et al., 2011; Madeira et al., 2015).

East of the Terceira Rift, the Eurasian-Nubian plate boundary is expressed by the GLORIA Fault, a right-lateral transform fault (Laughton et al., 1972; Argus et al., 1989; Verzhbitsky et al., 2011). The East Azores Fracture Zone, located from west of the GLORIA Fault towards east of the Mid-Atlantic Ridge, corresponds to an abandoned fault segment that probably represents the ancient limit of the Eurasian-Nubian boundary (Searle, 1980; Luis et al., 1994; Dias et al., 2007).

Despite the geodynamic setting, the magmatism of the Azores region is made considerably more complex as result of a possible hotspot, fed by an underlying mantle plume, and its interaction with the Mid-Atlantic Ridge (e.g. Schilling, 1975; White et al., 1976; Cannat et al., 1999; Gente et al., 2003; Montelli et al., 2004; Silveira et al., 2006; Yang et al., 2006; Beier et al., 2008).

A variety of evidence, including geochemical studies (Schilling, 1975; Flower et al., 1976; White et al., 1976; Bougault and Treuil, 1980; Schilling et al., 1983; Schilling, 1991; Dosso et al., 1999; Madureira et al., 2005; Millet et al., 2009; Beier et al., 2010) and geophysical observations (Luis et al., 1994; Detrick et al., 1995; Thibaud et al., 1998; Escartín et al., 2001; Silveira et al., 2006), have suggested the presence of a low seismic velocity melting anomaly in the mantle beneath the Azores Plateau. However, the origin, nature and location of the hotspot is still controversial. The anomalously thick crust of the oceanic Azores Plateau was probably formed 20 to 10 Ma ago due to the interaction between hotspot magmatism associated with the Azores mantle plume and rift magmatism from the Mid-Atlantic Ridge and the Terceira Rift (Cannat et al., 1999; Gente et al., 2003; Vogt and Jung, 2004; Yang et al., 2006; Beier et al., 2008; Georgen, 2011).

Up to date reviews on the geodynamic setting and its influence on the tectonics and magmatism of the Azores region can be found in Gente et al. (2003), Vogt and Jung (2004), Beier et al. (2008), Georgen and Sankar (2010), Verzhbitsky et al. (2011), Trippanera et al. (2013) and Madeira et al. (2015).

### 1.3. Occurrence of ignimbrites in the Azores islands

Ignimbrites, and other types of PDC deposits, are found on four of the nine islands of the Azores archipelago (São Miguel, Terceira, Faial and Graciosa). They are frequently associated with highly explosive eruptions from the active central volcanoes of those islands. Apart from specific studies on the ~30 ka Povoação Ignimbrite (Duncan et al., 1999) and the ignimbrites of the 4.5 ka Fogo A eruption (Pensa et al., 2015) on São Miguel, not much is known about the other ignimbrites and PDC deposits of the Azores.

The oldest dated ignimbrite in the Azores is Ignimbrite-i, on Terceira, with an age of approximately 86 ka (Gertisser et al., 2010). However, some of the undated Azorean ignimbrites may be close to or even older than 100 ka. On the other end, the youngest is the ignimbrite formed during the last major explosive eruption on Faial Island which occurred ~1000 years BP (Pacheco, 2001). In historical times, i.e. since the Portuguese settlement of the Azores in the 15<sup>th</sup> century, only the AD 1630 eruption of Furnas Volcano, on São Miguel, is known to have generated PDCs from a central volcano. At least 80 people were killed by the dilute density currents (i.e. pyroclastic surges; Cole et al., 1995).

The main pyroclastic formations containing ignimbrites and other PDC deposits found on each island are presented next, following the reviews on Caniaux (2015) and Gaspar et al. (2015):

On São Miguel Island, ignimbrites and PDC deposits occur on the three active central volcanoes (Sete Cidades, Fogo and Furnas), which are characterized by well-developed multi-phase calderas.

The volcanostratigraphy of Sete Cidades comprises three major pyroclastic formations that contain ignimbrites. They are interpreted to result from paroxysmal eruptions associated with different phases of caldera formation (Queiroz, 1997; Queiroz et al., 2008; Queiroz et al., 2015). From the oldest to the youngest: the Risco Formation (~36 ka) records the first caldera-forming event of Sete Cidades; the Bretanha Formation (~29 ka) is related to the second caldera collapse; and the Santa Bárbara Formation (~16 ka) is associated with the third and final paroxysmal event of caldera collapse. All three formations are dominated by ignimbrite members, but also include other members with

pumice fall and minor PDC deposits (e.g. pyroclastic surge and block-and-ash flow deposits). Two ignimbrite outcrops identified at Rocha da Relva and Ponta da Ferraria (Queiroz, 1997; Caniaux, 2015) are undated but interpreted to be older than the formations described previously.

In the last 5 ky, other minor PDC deposits related to the recent intracaldera activity of Sete Cidades are also recognized. From the 17 explosive eruptions that occurred inside the caldera (deposits P1 to P17), at least five have generated PDCs, which emplaced small and localized dilute PDC deposits. Among these, P1 is clearly distinct from all the others as it includes the thickest PDC deposit, known as the Candelária ignimbrite (Queiroz, 1997; Queiroz et al., 2008).

On Fogo Volcano (also known as Água de Pau), six major ignimbrite-bearing formations are recognized (Wallenstein, 1999; Wallenstein et al., 2015). Due to difficulties in establishing correlations, the stratigraphy of the north and south flanks of the volcano are described separately. The volcanic sequence of the north flank includes at least three formations that contain several ignimbrites and PDC deposits: the Porto Formoso Formation (~21 ka), the Chã das Gatas Formation (stratigraphically constrained between 21 and 19 ka) and the Barrosa Formation (its stratigraphic position is not established). Older (>40 ka) unnamed ignimbrites were also identified along the north coastal cliffs of Fogo (Wallenstein, 1999). The south flank sequence includes two pyroclastic formations with ignimbrites: the Roída da Praia Formation (from ~34 to ~15 ka) and the Ribeira Chã Formation (constrained between 12 and 8 ka). The latter was emplaced during a paroxysmal caldera-forming event (Wallenstein, 1999).

The Fogo A Formation (4.5 ka) outcrops both north and south of Fogo caldera (Wallenstein, 1999; Pensa et al., 2015). It corresponds to a paroxysmal Plinian eruption, associated with caldera formation, that generated different types of PDCs recorded by distinct deposits: dilute PDC deposits (i.e. pyroclastic surge deposits), intra-Plinian ignimbrites and a climatic ignimbrite (Pensa et al., 2015).

Furnas Volcano is characterized by a complex stratigraphy that includes at least six formations with several ignimbrites and other types of PDC deposits. Two of these ignimbrites are related to major caldera collapse events (Guest et al., 1999; Guest et al., 2015). The older ignimbrite-bearing formations of Furnas are: the Amoras Formation

(undated but stratigraphically constrained between 95 and 30 ka) and the Albufeira Formation (>44 ka). The latter is overlaid by the Quente block-and-ash flow deposit (Guest et al., 1999). Caniaux (2015) describes two other ignimbrites at Praia da Viola and north of Povoação village, but these are probably outcrops of ignimbrites from Amoras and Albufeira formations, respectively.

The Povoação Ignimbrite Formation (~30 ka) is a distinct welded deposit that records the largest eruption in the history of Furnas Volcano. It is interpreted to represent its first caldera-forming event, responsible for the collapse of the older Furnas caldera (Duncan et al., 1999; Guest et al., 1999).

Other pyroclastic formations located stratigraphically above the Povoação Ignimbrite also include ignimbrites, namely: the Ribeira do Tufo Formation (~27 ka), the Ponta Garça Ignimbrite Formation (~17 ka) and an unnamed younger ignimbrite (~12 ka) that outcrops below Pico do Ferro. The latter is believed to be associated with the collapse of the inner Furnas caldera (Guest et al., 1999). Within the Upper Furnas Group (<5 ka), a few dilute PDC deposits are associated with the AD 1630 (also known as Furnas J), Furnas I and Furnas C eruptions (Cole et al., 1999).

On Terceira Island, at least seven pyroclastic formations dominated by ignimbrites are recognized in the last 86 ky. The source of the associated PDC-forming events has been traced to the central part of the island, i.e. Pico Alto and/or perhaps Guilherme Moniz twin volcanoes (Self, 1974, 1976; Gertisser et al., 2010). The larger formations are named following the ignimbrite members that outcrop along the cliffs of the north and south coasts.

The lower formations in the stratigraphy include the Grota do Vale Ignimbrite Formation and the Pedras Negras Ignimbrite Formation. They are undated and found at the base of the south and north cliffs, respectively. Ignimbrite-i (~86 ka) is the oldest dated ignimbrite and corresponds to a small outcrop on the north coast. The other major formations have a wider distribution, generally occurring along both coasts: the Caldeira-Castelinho Ignimbrite Formation (dated at ~83 and ~71 ka), the Vila Nova-Fanal Ignimbrite Formation (dated between ~58 and >47 ka), the Linhares-Matela Ignimbrite Formation (~37 to ~35 ka), which is only seen in the southern part of the island, and the Lajes-Angra Ignimbrite Formation (~21 ka; Gertisser et al., 2010). Some ignimbrite-

bearing formations of Terceira are interbedded with pumice and/or ash fall deposits and occasionally debris flows, and are thought to be associated with caldera-forming events or periods. Other PDC deposits include the Quatro Ribeiras block-and-ash flow deposit and the Posto Santo spatter flow deposit (Gertisser et al., 2010).

The Lajes-Angra Ignimbrite Formation, one of the case studies in this thesis, is the most extensive ignimbrite formation on Terceira and has been used as the main lithostratigraphic horizon for the whole island. The Lajes and Angra ignimbrites were initially studied separately by Self (1974, 1976) and later grouped into the same formation by Gertisser et al. (2010). Figure 1.2 shows the Lajes Ignimbrite outcrop at the type location.



**Figure 1.2.** Outcrop of the Lajes Ignimbrite west of Lajes village (type location; scale is 1 m).

On Faial Island, ignimbrites and PDC-associated deposits have a reduced expression and only occur on Caldeira Volcano. Caldeira's eruptive history reveals 14 explosive eruptions, most of them produced small volume pumice and/or ash fallout and only two have generated PDCs (Pacheco, 2001). The C9 deposit (~1600 years BP) includes minor PDC deposits, mainly scattered on the north flank of the volcano, which correspond to Caniaux's (2015) Ribeira do Risco Ignimbrite.

The C11 deposit (~1000 years BP), the other case study in the thesis, records the last major explosive eruption on Faial. It is clearly distinct from the other deposits, as it is the only that includes a widespread ignimbrite (informally known as Cedros ignimbrite; Caniaux, 2012). The deposits of this eruption have been studied by Madeira (1998) and Pacheco (2001) and are associated with the formation of the volcano's caldera. Figure 1.3 shows the typical aspect of the C11 ignimbrite.



**Figure 1.3.** Outcrop of the (Cedros) ignimbrite of C11 south of Cedros village (scale is 1 m).

Only one PDC deposit has been identified on Graciosa Island. It is part of the Upper Hydromagmatic Sequence (~12 ka) of the Central Volcano, which is interpreted to result from a caldera-forming event (Gaspar, 1996).

In summary, ignimbrites and other PDC deposits are recurrent in the stratigraphy ( $\leq 100$  ka) of Azorean central volcanoes with calderas, except for Santa Bárbara Volcano (Terceira) and Caldeirão Volcano (Corvo). Most ignimbrites are associated with paroxysmal eruptions that led to caldera collapse events, however the genesis of some ignimbrites, particularly the older ones, is difficult to determine. Other types of PDC deposits (e.g. dilute PDC/surge deposits, block-and-ash flow deposits), result from a wide

range of eruptive styles, including intracaldera sub-Plinian eruptions, but can also be found as part of major pyroclastic formations related to caldera-forming eruptions.

The ignimbrites of the Azores are generally trachytic in composition, yet several have a mildly peralkaline nature (e.g. Terceira's ignimbrite suite). The presence of pumice/ash fall deposits at the base or the top of the ignimbrites (e.g. Povoação and Santa Bárbara ignimbrites), or conversely, the occurrence of intra-Plinian ignimbrites (e.g. Fogo A) reflect significant changes in eruptive style. It suggests that most ignimbrites result from PDCs generated by unsteadiness of the eruption column, that lead to total or partial collapses, or even alternation of convective and collapsing regimes.

Most ignimbrites outcrop along the coastal cliffs of the islands and are poorly available on land, except for the younger and the best exposed ones (e.g. C11's Cedros ignimbrite, Fogo A and Lajes-Angra Ignimbrite formations). In particular, some of the older ignimbrites are only seen in certain locations at the base of the cliffs. Given the short distances between calderas and coastlines at the Azores islands, it is believed that large volumes of ignimbrite are deposited offshore. Thus, the true ignimbrite volumes are unknown or, perhaps, substantially underestimated. Nevertheless, the larger ignimbrites probably did not exceed 1 km<sup>3</sup> DRE volume (Gertisser et al., 2010; Caniaux, 2015).

The distribution of various ignimbrites reveals that PDCs recurrently deposit on the same areas of the islands and follow similar flow paths. This is evident when grabens and deep dissecting valleys are found in the vicinity of central volcanoes (e.g. Fogo and Caldeira volcanoes, in São Miguel and Faial islands, respectively). These observations suggest the existence of preferential sectors or recurring paths for PDCs, which should be considered as vulnerable areas for future eruptive events (Caniaux, 2015). These flat (due to the ignimbrite surfaces) lowlands have, of course, been preferred areas for human occupation.

## 1.4. Thesis objectives

The main goal of this thesis is to improve the overall understanding of explosive volcanic eruptions, in particular of those that occur in the Azores and produce PDCs. To achieve this goal, two contrasting types of PDC-forming episodes from central volcanoes of the islands of Terceira and Faial were studied in detail. These studies allow a comprehensive understanding of the wide range of eruptive styles that produce PDCs and how the dynamics of these currents varies through time and space.

The specific objectives common to both case studies presented in the thesis are:

- (1) To define the distribution of the various volcanic products;
- (2) To describe and interpret the different lithofacies and their vertical and lateral variations;
- (3) To constrain the transport and depositional processes acting in the PDCs;
- (4) To determine the physical parameters of the eruptions;
- (5) To use physical volcanology to interpret eruption histories and styles;
- (6) To characterize the petrography, mineralogy and geochemistry of the juveniles products;
- (7) To determine the magmatic intensive parameters;
- (8) To constrain magmatic processes occurring in the reservoirs.

## **1.5. Studied volcanic deposits**

Previous studies on ignimbrites and PDC deposits of the Azores have shown that they can result from various eruptive styles and are frequent on different evolutionary stages of Azorean central volcanoes, usually during paroxysmal eruptions associated with caldera-forming events (Walker and Croasdale, 1971; Self, 1974, 1976; Booth et al., 1978; Gaspar, 1996; Queiroz, 1997; Duncan et al., 1999; Guest et al., 1999; Wallenstein, 1999; Pacheco, 2001; Gertisser et al., 2010; Caniaux, 2015; Pensa et al., 2015, among others).

As seen earlier, Terceira Island has a long record of ignimbrite formations, making it the Azorean island with the largest volume of ignimbrite. The youngest of these ignimbrite-dominated formations, the Lajes-Angra Ignimbrite Formation with an age of approximately 21 ka, was chosen as a case study because: (1) it records one of the largest PDC-forming events in the Azores; (2) is one of the best exposed ignimbrite formations of the archipelago, with extensive outcrops along the coasts of Terceira; (3) it includes one of the first examples of a low-aspect ratio ignimbrite in the literature, the Lajes Ignimbrite (Walker et al., 1980); and (4) it exhibits a relatively rare peralkaline composition.

Explosive volcanism on Faial Island is fairly recent (<16 ka) and restricted to Caldeira Volcano. Among the deposits of explosive eruptions, the C11 deposit of the ~1000 years BP eruption was selected as the other case study because: (1) it is the last major PDC-forming eruption in the Azores; (2) it is associated with the youngest caldera collapse of an Azorean central volcano; (3) there are a large number of outcrops making it widely accessible at the surface; and (4) the pristine nature of the deposits allows the use of various methods for the characterization of the products.

Although the two selected case studies include extensive ignimbrites, with somewhat similar lithofacies, the deposits record eruptive styles with distinct magmatic compositions, eruptive histories and emplacement processes. These deposits are thought to represent very different PDC-forming episodes from Azorean central volcanoes. Furthermore, the study enables comparisons of interpretations that are possible by working on both recent and older deposits.

## **1.6. Methods of study**

The work presented here started with extensive field work in the islands of Faial and Terceira. Field studies of the selected deposits integrated geological mapping with detailed reconstruction of stratigraphic sections, including description of lithofacies and their vertical, lateral and longitudinal variations. Major unconformities such as palaeosols and/or erosion surfaces were used to delimit the deposits. A lithofacies based approach was used to obtain an overall understanding of the eruptive and depositional processes. This approach has been successfully applied to other complex pyroclastic deposits and ignimbrites (e.g. Sohn and Chough, 1989; Allen and Cas, 1998; Brown and Branney, 2004; Brown et al., 2007; Sulpizio et al., 2007).

Field work was complemented by various analytical methods. Grain size and component analyses of the deposits were performed following the methodology of Cas and Wright (1987). The morphology of juvenile ash was examined by means of scanning electron microscope (SEM) images.

Petrographic and modal analyses were carried out by thin-section observation under the binocular microscope. Major and trace element whole-rock geochemical analyses were performed by fusion inductively coupled plasma (FUS-ICP) and inductively coupled plasma mass spectrometry (ICP-MS), respectively, in a commercial laboratory (Activation Laboratories Ltd., Ontario, Canada). Electron microprobe analyses were carried out on the main mineral phases and groundmass glasses. Further details on the different methodologies used are discussed in the appropriate chapters.